SciMedCentral

JSM Chemistry

Research Article

Significance of Proline Residue on Short Mucin Peptide Interactions with Mouse MUC1 Monoclonal Antibody Studied by Saturation Transfer Difference NMR Spectroscopy

Cheng Her[1], William M. Westler[2] and Thao Yang[1]*

[1]*Department of Chemistry, University of Wisconsin – Eau Claire, USA*
[2]*Department of Biochemistry,University of Wisconsin, USA*

***Corresponding author**
Thao Yang, Department of Chemistry,University of Wisconsin – Eau Claire, 105 Garfield Ave, Eau Claire, WI 54702, USA, Tel: 715-836-4190; Fax: 715-836-4979; Email: yangt@uwec.edu

Submitted: 01 October 2013

Accepted: 15 October 2013

Published: 17 October 2013

Copyright

© 2013 Yang et al.

OPEN ACCESS

Keywords

- MUC1 antibody recognition epitope
- Mucin peptide
- Saturation Transfer Difference NMR Spectroscopy (STD NMR)

Abstract

In this study we investigated to see whether or not a shortened MUC1 mucin peptide epitope with the sequence GVTSAPD containing a single prolyl residue would still bind specific monoclonal antibody as its native sequence (e.g., PDTRP), known to be the specific recognition site on the Variable Number Tandem Repeat (VNTR) region of MUC1 mucin by the immune system. The affinity of GVTSAPD peptide to a mouse Muc1 mucin specific monoclonal antibody (clone 6A4, IgG1 isotype) was investigated by Saturation Transfer Difference NMR spectroscopy (STD NMR). Results showed that the shortened mucin epitope GVTSAPD still retained affinity to Muc1 specific monoclonal antibody (mAb) while one that lacks the prolyl residue at position 6 lost its affinity, which suggests that P_6 is necessay for antibody binding. The interactions observed by STD NMR occurred strongest at the P_6 side chain ^{1}H's (βH and γH); the P_6H_α showed lower degree of saturation transfer effect. Minor interactions also occurred at the methyl groups of V_2, T_3 and A_5. Mucin peptides derived from the VNTR region have been the target of cancer vaccine research, thus properties associated with mucin peptide structure, conformation and antibody interaction are central to peptide design or engineering towards that end.

ABBREVIATIONS

DCM: Dichloromethane; DIPEA: Diisopropylethylamine; DMF: Dimethylformamide; Fmoc: N-α-9-fluorenylmethoxycarbonyl; Fmoc-Asp(OtBu)-Wang resin (100-200 mesh): N-α-Fmoc-L-aspartic acid β-t-butyl ester-Wang resin; HB: Hydrogen Bond; HBTU : O-(Benzotriazol-1-yl)-N,N,N',N'-tetramethyluronium hexafluorophosphate; HOBt: N-hydroxybenzotriazole; mAb : monoclonal antibody; SDS-PAGE: Sodium Dodecylsulfate Poly-acrylamide Gel Electrophoresis; Wang resin: *p*-alkoxybenzyl alcohol-linked Wang resin

INTRODUCTION

The antibody binding study of a shortened MUC1 mucin peptide epitope derived from the Variable Tandem Repeat domain (VNTR) of MUC1 mucin to a mouse Muc1 mucin specific monoclonal antibody (isotype IgG1, clone 6A4) was investigated by Saturation Transfer Difference NMR (STD NMR) spectroscopy. MUC1 mucin is a large molecular weight (> 400 kDa) glycosylated protein tethered to a transmembrane C-terminal domain (MUC1-C) on the cell surface expressed by glandular and ductal epithelial cells [1,2]. Most human adenocarcinoma epithelial cells, including those from breast and ovary overexpress a form of MUC1 mucin that is aberrantly glycosylated causing exposure of peptide backbone and cryptic oligosaccharide chains that exhibit antigenic properties, which make them novel target species for cancer therapy [1,3]. Some hematopoietic cells also produce MUC1 mucin, for further review see references 4 and 5 [4,5]. The role of MUC1 mucin is diverse, ranging from lubrication and/or hydration of epithelial cell surfaces, protection against invasion of pathogens and acidity, involved in embryonic implantation, epithelial sheet formation and morphogenesis, cell-cell interactions, intracellular cell signaling that promote growth and transformation, to immune regulation [6-9]. MUC1

Cite this article: Her C, Westler WM, Yang T (2013) Significance of Proline Residue on Short Mucin Peptide Interactions with Mouse MUC1 Monoclonal Antibody Studied by Saturation Transfer Difference NMR Spectroscopy. JSM Chem 1(1): 1004.

mucin in tumor cells is immunosuppressive, the overproduction of it masses tumor cell surfaces, inhibiting cell lysis, promoting their growth and metastatic progression [10,11], thus affirming an evidence for rendering the immune system ineffective in countering against tumor growth. Cryptic peptide epitopes dispersed into the circulation or microenvironment of tumor have been known to induce cellular and humoral immune responses to MUC1 mucin [12,13]. A well known 20-amino acid (20-aa) MUC1 epitope residing at the VNTR domain which comprises the sequence GVTSAPDTRPAPGSTAPPAH is an immunodominant sequence recognized by the immune system either as naked peptide or glycosylated peptide [14-16]. The x-ray crystal structure of a breast cancer specific monoclonal antibody (clone SM3) that recognizes the immunodominant sequence (a 13-aa peptide, TSAPDTRPAPGST) has been determined [17]. The peptide is bound in an extended structure with most of the interactions (vdW contacts, direct HB or water mediated HB) between the antigen peptide and the antibody occurring at the N-terminal end located at the APD region [17]; most interactions are of hydrophobic nature. Several MUC1 mucin peptide - antibody binding studies in solution by NMR had been carried out, for further review see [18-24]. Of direct relevance to this investigation are the studies carried out by Grinstead et al. [21] and Möller et al. [22]. Grinstead and coworkers carried out a binding study of a 16-aa and a 20-aa MUC1 mucin peptides and the antibody Fab fragment by ^{15}N and ^{13}C NMR relaxations of the peptides. These workers showed that the peptide domain that was immobilized was located at the entire domain PDTRPAP within the 20-aa VNTR domain, and that the preceding and subsequent sequences of the MUC1 mucin peptides were unbound and flexible in solution. The investigation by Möller et al. [22] using a 5-aa MUC1 mucin peptide PDTRP and a glycopteptide PDT(O-α-D-GalNAc)RP binding to antibody SM3 by STD NMR showed that the interactions between the PDTRP peptide and the antibody was strongest at the P_1 residue and dropped off sequentially at residues 2-5; similarly the P_1 residue had the strongest binding effect in the PDT(O-α-D-GalNAc)RP peptide, in contrast, residues 2-5 had similar binding strength. In addition, the GalNAc residue showed a strongest binding at the methyl group comparable to that of the P_1 residue, whereas the rest of the GalNAc ring protons (CH protons) showed considerable binding effects but lower in degree of saturation effect compared to those observed for residues 2-5.

The single and main epitope sequence that is well-defined and accepted to be that which is recognized by monoclonal antibody is the 5-aa sequence PDTRP [17,21]. Therefore, most mucin peptide-antibody binding cases have focused on that main epitope. In this investigation we are interested to probe the binding activity of MUC1 mucin peptide with sequence that lies slightly outside of the main epitope (i.e. PDTRP). The Muc1 antibody (mouse IgG1 monoclonal antibody, clone 6A4 from Genway Biotech) is an antibody that recognizes the sequence SAPDTRPA. We chose to use the 7-aa sequence GVTSAPD that resides at the N-terminal region of the main epitope to see if it would still be recognized by the specific monoclonal antibody expressed against the main binding epitope. In addition, we wanted to evaluate the critical groups on a particular residue or a residue necessary for binding. Thus, position 6 was selected to be the mutation point. The first mutant peptide used has P_6 substituted by D_6 (i.e., GVTSADD). It is logical that in order to be successful in developing a mucin peptide-based vaccine, the antigenic agent must be able to induce humoral responses to such agent. The mere binding of mucin peptide to antibody does not ensure that an effective immune response against tumor mucin or tumor cells will develop. Hence, it would not be illogical to explore variety of antigenic agents, including peptides with altered sequences, or cyclic peptides, glycopeptides, glyco-lipopeptide complex [25,26], and combination of multivalency glycoconjugates, which constitute the latest antigenic agents being designed [27]. Undertanding which amino acid residue or which group of protons on the mucin peptide is essential for binding antibody will be one of the crucial bases for designing antigenic agents. Herein, we report the interactions of a shortened MUC1 mucin peptide GVTSAPD to a specific Muc1 monoclonal antibody versus one that lacks binding (e.g. GVTSADD).

The STD NMR results showed that the protons of the methyl groups of V_2, T_3 and A_5 have interactions with the antibody, but other protons of these three residues have essentiall no binding effect. Significant interactions are centered at the protons of the P_6 residue. Based on the fact that all its protons received saturation transfer effect unlike other residues, it may be concluded that the P_6 residue is a critical residue in the peptide's structure and ability for interacting with the antibody.

MATERIALS AND METHODS

Chemicals and reagents

Fmoc-amino acids, DIPEA, HBTU and HOBt were purchased from Peptide International and Advanced Chem Tech; pre-loaded resins (Fmoc-Asp(OtBu)-Wang, from Novabiochem; DMF, DCM, ether, acetonitrile, from ACROS Organics/Thermo Fisher Scientific; piperidine, hydrazine, TFA, from Sigma-Aldrich; salts and phosphate buffer, from Mallinckrodt Baker Inc.; Kaiser test reagents, from AnaSpec Inc.; NMR solvents, from Cambridge Isotope Laboratories Inc.; NMR tubes, from Wilmad LabGlass and Norell Inc.; Muc1 monoclonal antibody (6A4), from GenWay Biotech.

Peptide synthesis

Peptide was synthesized manually via Fmoc chemistry [28]. The pre-loaded resin (0.1 mmole, Fmoc-Asp(OtBu)-Wang 100-200 mesh, 0.58 mmole/g) was put in a reaction vessel and pre-washed with DMF once or twice, then swollen in DMF for 5-10 min. The Fmoc-group was removed using freshly prepared 20% (v/v) piperidine in DMF for 20 min. After deprotection of the Fmoc-group and the excess piperidine drained, the resin was washed with a cycle of DMF (3x), DCM (1x), and DMF (3x); each wash with 5 mL of solvent for 0.5 min. Coupling was carried out for 1h at room temperature with 1.25 equivalent of DIPEA as base for deprotonation of the α-carboxylic acid group, 4x excess (0.4 mmole) of Fmoc-amino acid and 4x excess of the coupling reagents HBTU and HOBt. All reagents were dissolved together in 3 mL of DMF. At the end of the coupling reaction, the excess Fmoc-amino acid and reagents were drained, and the peptidyl-resin was cleaned with a cycle of DMF (2x), DCM (1x), and DMF (2x); each wash with 5 mL of solvent for 0.5 min.

For peptide cleavage, after the last Fmoc-group was removed, the peptidyl-resin was cleaned with 5 mL of DMF (3x) and DCM (3x), evacuated to dryness, then the peptide was cleaved using minimal amount of 95% TFA-water mixture for 2h. Crude peptide in 95% TFA was collected into a round bottom flask; the excess TFA was evaporated to minimal volume (~1 mL), then precipitated by 20-50x volume of cold diethyl ether. The precipitated crude peptide was allowed to settle, transferred to 50 mL centrifuge tube and centrifuged to pack it (Beckman J2-HS centrifuge). The peptide was ether-washed (3x) with excess volume of ether; each time followed by centrifugation and aspiration of the ether solvent. Following the ether wash, the crude peptide was dissolved in minimal amount of deionized water (3-10 mL) and its aqueous layer washed again with ether (3x). Finally, the dissolved crude peptide was frozen and lyophilized to dryness (Labconco Freeze Dry System) and kept in -80 °C freezer for subsequent HPLC purifications.

Peptide purification

Peptide was purified via reverse phase HPLC (RAININ HPXL Solvent Delivery System) using a gradient elution of solvent A [98.9% water, 1% acetonitrile (ACN), 0.1% TFA] and solvent B (99% ACN, 0.9% water, 0.1%TFA) [29]. A Varian Pro Star PDA UV-VIS system was used for detection of peptide at 220 nm and 280 nm. For purification, the differential migration of the desired peptide from impurities was achieved using a protein and peptide Grace Vydac C_{18} silica-based HPLC column (218TP1010, 10µm, 10x250mm); for analytical purpose, an analytical Grace Vydac C_{18} silica-based HPLC column (218TP54, 5µm, 4.64x250mm) was used. A linear gradient of 5 – 30% solvent B was used for elution of peptides in each run for 40 minutes.

Mass spectral analysis

Mass spectra were acquired by an Electro-Spray Ionization Time-of-Flight (ESI-TOF) LC/MS spectrometer (Agilent 6210 Time-of-Flight LC/MS), in which the sample was analyzed over a C_{18} column prior to being electrosprayed into the mass spectrometer [30]. The LC part was carried out using an Agilent C_{18} (Eclipse XDB-C_{18}, 5 µm, 4.6 x 150 mm, LN B06072) column with a flow rate of 0.5 mL/min, and a temperature of 23 °C at the left end and 22 °C at the right end of the column. The Total Ion Current (TIC) was used to characterize the retention time of the peptide sample. For the LC, solvent A contained 99% H_2O, 1% MeOH, 1 mM ammonium acetate, and solvent B contained 99% MeOH, 1% H_2O, 1 mM ammonium acetate. The pH of both solvents were adjusted to pH 5. A volume of 5 µL of peptide sample was injected in each run. The LC run was carried out with a gradient of solvent B initially at 5%, ramped to 100% linearly at 0-11 min., held constant at 100% B for 4 min., then decreased linearly back to 5% in 1 min. and flushed for another 4 min. before the run ends at 20 min. A post-run time of 4 min. at 5% B was also used between each run.

For the MS part, the ESI technique with a positive or negative ion polarity mode was employed with a mass range at 100-3,000 m/z. The parameters for mass spectral acquisition were set to: 5025 transients/scan, 0.93 cycles/sec, gas temperature at 350 °C, flow rate of drying N_2 gas at 12 L/min., nebulizer pressure of 45 psig, capillary of 4,000 V, fragmentor at 225 V, skimmer at 60 V, OCT RFV of 250 V, and ion energy of -37.0 V. Masses were externally calibrated with the ES-TOF tuning mix solution of Agilent (pat No. G1969-85000), which contains 10 reference masses. The allowable mass error from the mass calibration is ± 2 ppm.

NMR spectroscopy

NMR experiments were run with peptide sample concentrations of 2-3 mM in 20 mM phosphate buffer, 5 mM NaCl, 90% H_2O, 10% D_2O, at pH 5 (uncorrected for deuterium effect). NMR data were collected by a Bruker 400 MHz (9.3977 T) NMR spectrometer with a triple-resonance inverse detection probe (TXI 400SB H-C/N-D). 2D NMR data were acquired with standard pulse sequences of TOCSY and ROESY [31], using a spectral width window of 13 ppm (5028.3 Hz), F_n mode of States-TPPI, and a delay of 2 s prior to acquisition. The 2D TOCSY employed a Hartman-Hanh transfer MLEV-17 pulse sequence with a spin-lock of 60 ms and a trim pulse of 2.5 ms; the 2D ROESY was employed with a continuous wave spinlock for mixing, typically 300 ms, but several experiments were run with spinlock of 70-400 ms for comparison of data. The 2D ROESY NMR data used in this work were from those acquired at mixing time of 300 ms. All 2D data were acquired with phase sensitive mode; the HDO suppression was achieved by the water suppression pulse sequence 3-9-19 WATERGATE [32]. Typical 2D NMR data contained 32 transients and a size of 2k x 0.5k. 2D NMR data were processed by the iNMR software [33] with zero filling in the t_1 dimension to 1k, typically a size of 2k x 1k was used. The Sparky software [34] was used to make proton assignments. All chemical shifts were referenced to the HDO signal at 4.97 ppm at 7 °C.

For 1D STD NMR experiments, the samples contained 0.016 mM of mouse Muc1 IgG (6A4 clone, M_r 122 kDa), 1.0 mM of MUC1 peptide with a peptide:protein ratio of 62.5:1.0 (sometimes at a ratio of 100:1), in 20 mM phosphate buffer, 5.0 mM NaCl, 100 % D_2O, pH 7 at 7°C. The mouse Muc1 specific monoclonal antibody 6A4 that recognizes the epitope SAPDTRPA within the core 20-aa Tandem Repeat on MUC1 mucin was used as supplied without further purification. The monoclonal antibody is of the isotype IgG1 (clone 6A4) from hybridization of FO myeloma cells with spleen cells from Balb/cj mice (Genway Biotech, Inc.). The Muc1 antibody was greater than 95% purity by SDS-PAGE, and has a concentration 2.58 mg/ml (0.388 mL). Protein concentration, retention and buffer exchange was achieved by ultra centrifugation unit (Millipore Amicon Ultra-4 Centrifugal Filter Unit).

The 1D STD NMR data were acquired by the 40 Gaussian shaped pulse train for saturation on the f2 channel alternating between on and off resonance [32,35-38]. The 1D STD pulse sequence is: relaxation delay, presaturation pulse train, π/2-pulse, spin lock (if applicable), then acquisition. The pulse sequence uses selective presaturation of 40 Gaussian shaped pulses of 50 ms, with 1 ms delay prior to the π/2-pulse. Total saturation time was 2.00 s with a relaxation delay of 2.10 s. Separate STD NMR spectra were also acquired with the spoil pulse sequence to destroy unwanted magnetization, water suppression using excitation sculpting with gradients and spinlock (30 ms) to suppress the broad protein background (Bruker pulse sequence std diff esgp.3) [32]. The spin lock and trim pulse (30 ms) were

set immediately after the π/2-pulse with power level of 0.259 W during the trim pulse and spin lock [32,36]; other parameters and conditions were the same as the non-excitation sculpting pulse sequence. The irradiation power during the presaturation pulse train was 0.0356 mW for all the STD NMR experiments. The 1D STD NMR data were recorded as serial pseudo 2D data. The on-resonance FIDs and off-resonance FIDs were split, multiplied by the same factor but with a negative factor applied to the off-resonance FIDs after acquisition, then summed. The resultant difference FID is the STD FID; it was then transformed to the STD NMR spectrum. The on-resonance frequency was set at either -2 ppm or 7 ppm where there is no ^{1}H resonances arise from the peptide ligand at or near these frequencies, but ^{1}H resonances exist for the antibody at these frequencies. The off-resonance frequency was set at 40 ppm. Both set of data for on-resonance frequency set at 2 ppm and 7 ppm were collected for each pulse sequence. The data were typically recorded with 32 dummy scans, 1024 scans by 512 t1 points with a spectral window of 5028.3 Hz, at 7 °C. Control STD NMR spectra were carried out with the corresponding peptide at the same concentration using the same pulse sequence and parameters without the antibody to make sure that there was no spurious saturation transfer peaks due to excessive saturation power. All conditions and spectral parameters used on the peptide-antibody mixture were the same as those that resulted in a flat STD NMR spectrum for the control peptide.

Temperature Coefficient Measurement. The temperature dependent of the NH's of the peptide was measured by 1D NMR using the peptide concentration of 2-3 mM, in 20 mM phosphate buffer, 5 mM NaCl, 90% H_2O, 10% D_2O, pH 5 with variable temperature from 7-45 °C. The data were acquired with a spectral window of 4800 Hz, 64 scans, 16 dummy scans, and a delay of 2 s. The pH was uncorrected at high temperatures. The HDO resonance was suppressed by the WATERGATE 3-9-19 pulse sequence [32]. Sample temperature was incremented by 5 °C apart per spectrum, except for the first two points from 7-10 °C. Temperature was allowed to equilibrate for 10 min., and probe condition was re-optimized by new lock, tuning and shimming before data points were acquired. 1D NMR spectra were typically processed with a 0.3 Hz linebroadening directly by TopSpin (v 2.0.5) on an off-station computer (PC). The HDO resonance of each spectrum of the sample at a specified temperature was referenced to a corresponding HDO resonance of a temperature-calibrated water sample (90% H_2O, 10% D_2O, pH 5) at that same temperature. Temperature dependent of NMR spectral characteristics of the peptide amide ^{1}H's in aqueous environment was used to estimate the temperature coefficient [39].

RESULTS AND DISCUSSION

Peptide synthesis, HPLC purification and mass spectral analysis

Peptide was synthesized by the solid-phase technique via usual Fmoc-chemistry. The crude yield is 70 - 85%. Peptide was purified to ≥ 95% by HPLC prior to use. LC-MS analysis of GVTSAPD peptide showed an average isotopic mass of $[M + H]^+$ of 646.54 u compared to 646.66 u, theoretical mass, with the $[M + Na]^+$ of 668.39 u and the $[M + K]^+$ of 684.36 u (data not shown); for the GVTSADD peptide a mass of $[M + H]^+$ of 664.28 u was observed versus a theoretical mass of 664.63 u, with the $[M + Na]^+$ of 686.27 u (data not shown).

NMR results

The TOCSY 2D-NMR data were used for ^{1}H assignments, and the ROESY 2D-NMR data, for detection of spatial interproton distances ($d_{H-H} \leq 5$ Å). Assignments for the protons were achieved completely, except for the degenerate geminal αH's of G_1, and βH's of S_4; no stereospecific assignments were made. Table 1shows the ^{1}H chemical shifts assigned for GVTSAPD; and (Table 2), the ^{1}H chemical shifts assigned for GVTSADD.

For the GVTSAPD peptide, the amide temperature coefficients of all residues (Table 1), except that of G_1 which could not be estimated, were all more negative than -4.6 ppb/K (a value indicative of a buried NH involved in hydrogen bonding) [40,41]; the values suggest all NH's are accessible to solvent and that the peptide has no unique signature conformation, but an extended structure. For the GVTSADD peptide, all amide temperature coefficients were also more negative than -4.6 ppb/K (Table 2) except that of D_7, in addition a medium nOe was observed at D_6NH-D_7NH, which may indicate a turn-like structure and inaccessibility to solvent at D_7NH.

The STD NMR results showed that the linear peptide GVTSAPD has binding to the Muc1 monoclonal antibody 6A4 despite it containing only one prolyl residue and being an upstream sequence of the normal binding epitope PDTRP in the VNTR domain. (Figure 1) shows the STD NMR spectra of GVTSAPD peptide-Muc1 antibody mixture (traces D and E) compared to control spectra (Traces B and F). The STD NMR data showed that there are saturation transfer effect to the methyl groups of V_2, T_3, and A_5. The βH-region showed saturation transfer effect to the side chain protons of P_6 and a minor effect at D_7 (Figure 1, Trace E). The STD peak intensities of the rest of the βH's (V_2, T_3 and S_4) were essentially zero and their percent STD were not estimated.

Table 1: ^{1}H chemical shifts (ppm) of mucin peptide GVTSAPD (3 mM) acquired in 20 mM phosphate, 5 mM NaCl, 90% H_2O, 10% D_2O, pH 5.0, at 7 °C in the absence of monoclonal antibody.

Residue		Chemical shifts in ppm		Others	NH, Δδ/ΔT, (ppb/K)
	NH	αH	βH		
G		3.887			
		3.840[a]			
V	8.644	4.253	2.118	γ,γ'CH_3 0.955, 0.938	-6.2
		4.248	2.122	0.964, 0.946	
T	8.491	4.422	4.231	γCH_3 1.209	-8.6
		4.429	4.248	1.216	
S	8.464	4.439	3.842		-7.6
		4.429	3.768, 3.753		
A	8.476	4.614	1.367		-8.2
		4.618	1.373		
P		4.422	2.257, 1.993	γH 1.993, δ,δ'H 3.657, 3.790	
		4.429	2.270, 2.009	2.009, 3.630, 3.537	
D	8.119	4.366	2.619, 2.715		-8.3
		4.306	2.656, 2.511		

[a] Chemical shift values of second row under each residue were acquired in 20 mM phosphate, 5 mM NaCl, 100% D_2O, pH 7, at 7 °C in the presence of monoclonal antibody.

Table 2: ^{1}H chemical shifts (ppm) of mucin peptide GVTSADD (3 mM) acquired in 20 mM phosphate, 5 mM NaCl, 90% H_2O, 10% D_2O, pH 5.0, at 7 °C in the absence of monoclonal antibody.

Residue		Chemical shifts in ppm		Others	NH, Δδ/ΔT, (ppb/K)
	NH	αH	βH		
G		3.881			
		3.906[a]			
V	8.362	4.247	2.120	γ,γ'CH_3 0.956, 0.939	-5.7
		4.249	2.151	0.975, 0.967	
T	8.487	4.330	4.247	γCH_3 1.211	-7.6
		4.484	4.277	1.231	
S	8.487	4.330	3.886, 3.844		-7.6
		4.484	3.916, 3.854		
A	8.487	4.325	1.387		-7.6
		4.351	1.406		
D	8.402	4.702	2.886, 2.746		-5.3
		4.656	2.785, 2.535		
D	8.052	4.563	2.839, 2.839		-4.1
		4.359	2.666, 2.596		

[a]Chemical shift values of second row under each residue were acquired in 20 mM phosphate, 5 mM NaCl, 100% D_2O, pH 7, at 7 °C in the presence of monoclonal antibody.

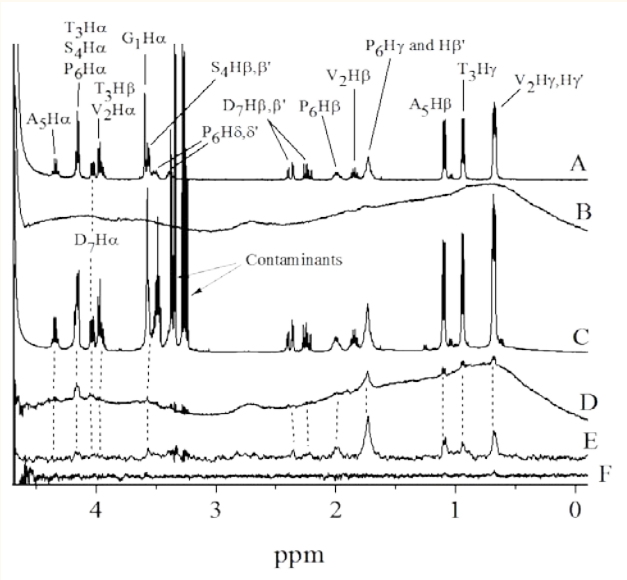

Figure 1 STD 1D ^{1}H NMR data showing the protons from the linear GVTSAPD peptide directly binding to monoclonal antibody (mAb) 6A4 in 20 mM phosphate, 5 mM NaCl, pH 7, 100% D_2O at 7 °C. The traces are: A). 1D ^{1}H NMR spectrum of linear peptide GVTSAPD in the absence of antibody (6A4, mAb); B). STD NMR spectrum of mAb in the absence of peptide showing broad-hump unresolved resonances indicative of efficient saturation transfer effect throughout the protein as a control spectrum; C). 1D ^{1}H NMR spectrum of a mixture of mAb and linear peptide GVTSAPD showing the ^{1}H resonances of the peptide riding on top of the unresolved resonances (broad-hump) of mAb (16 μM mAb, 1000 μM peptide); D). STD NMR spectrum of GVTSAPD plus mAb mixture showing mostly the STD effect of ^{1}Hs of P_6 residue that are directly bound to the mAb and some STD effect from the -CH_3 groups of V_2, T_3, and A_5 on top of the broad-hump mAb resonances; no protein background suppression on this spectrum; huge impurities resonances that do not bind to mAb do not show up as STD effect; spectrum was processed with a line broadening of 1.0 Hz and intensities were enhanced for visibility; E). Same STD NMR spectrum as in (D) but ran with protein background subtraction in order to see the STD effect better; note the huge contaminants in (C) do not bind to the mAb, thus are all subtracted out (in spectra D and E); dashed lines signify STD peaks; spectrum was processed with a line broadening of 1.0 Hz and intensities were enhanced for visibility; F). STD NMR spectrum of GVTSAPD peptide in the absence of mAb as a control spectrum; there is no mAb-peptide interactions, so no STD peaks resulted.

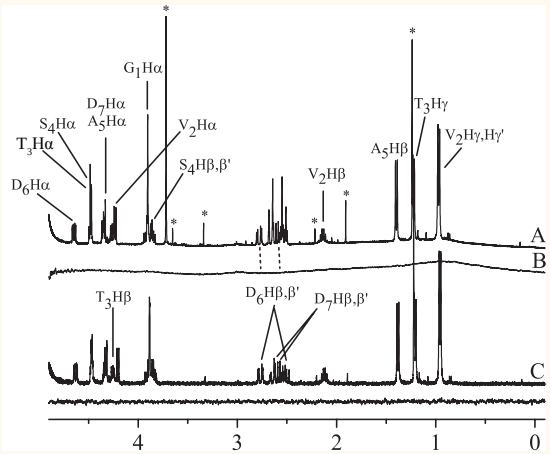

Figure 2 STD 1D ^{1}H NMR data showing the result of saturation transfer effect from mAb (6A4, mAb) onto the linear peptide GVTSADD in 20 mM phosphate, 5 mM NaCl, pH 7, 100% D_2O at 7 °C. The traces are: A). 1D ^{1}H NMR spectrum of a mixture of mAb and linear peptide GVTSADD showing the ^{1}H resonances of the peptide riding on top of the unresolved resonances (broad-hump) of mAb; B). STD NMR spectrum of GVTSADD and mAb mixture (16.4 μM mAb, 1000 μM peptide) showing no STD peaks on top of the broad-hump protein resonances because the protons of the peptide do not have any interactions with the antibody; C). 1D ^{1}H NMR spectrum of linear peptide GVTSADD in the absence of antibody; D). STD NMR spectrum of GVTSADD peptide in the absence of mAb as a control spectrum; there is no mAb-peptide interactions, so no STD peaks resulted. Sharp peaks marked with stars (*) are contaminants.

Table 3: The percent areas of STD peaks relative to the corresponding non-saturated transferred resonance peak areas. The values represent percent area of STD peaks to the corresponding peaks without saturation.

Residues	αH	βH	γH	δH
G	1.1			
V	_	0	1.3	
T	_	_	1.2	
S	_	_		
A	_	1.9		
P	1.6	4.5	7.1	_
D	_	2.0		

(_) percent STD was not estimated.

The STD NMR peak intensity is strongest at P_6H_δ (Traces D and E). The αH-region showed bigger saturation transfer effect to the P_6 and minor effect to the D_7.

Figure 2 shows the STD NMR results for the GVTSADD peptide-Muc1 monoclonal antibody binding study. The spectrum showed broad humps indicative of the saturation transfer effect on the antibody only (Figure 2, Trace B); no STD peaks were observed corresponding to any of the resonances of the peptide, which is indicative of no interaction between the protons of the peptide and the antibody. A separate STD NMR spectrum ran with the spoil pulse sequence using excitation sculpting with gradients and spinlock (30 ms) to suppress the broad protein background resulted in a flat line (data not shown); thus, no interaction occurred between GVTSADD and the antibody (mAb 6A4).

Table 3 shows the percent STD peak area for each type of side chain protons (Figure 1, Trace E) extracted relative to the

peak area of the corresponding protons on a control spectrum (Figure 1, Trace C) for GVTSAPD. The values represent percent areas of each STD peak relative to the corresponding peak area without the STD effect. Most significant saturation transfer effect occurred on the protons of P_6. For P_6 residue, the percent STD of the γH and βH peak overlapping together is 7.1%; for a second βH, 4.5%; and for the αH, 1.6%. The percent STD of the δH's of P_6 was not estimated due to overlapping with the huge contaminant peaks from the antibody sample sitting on top of them. The percent STD of CH_3-groups of A_5, T_3 and V_2 were estimated to be 1.9%, 1.2% and 1.3%, respectively. Saturation transfer effect to the protons of S_4H_β was too small and not estimated, but for G_1H_α and D_7H_β, their effects were 1.1% and 2.0%, respectively.

Several protons on the GVTSAPD peptide showed interactions with the Muc1 monoclonal antibody 6A4 as indicated by the rising STD peaks corresponding to the individual peaks on the peptide, whereas the peptide lacking the prolyl residue at position 6 showed no proton interactions with the antibody. However, the STD peak intensities observed for the α-protons were very weak, except for the peak where the αH of P_6 is centered, which showed stronger intensity but is still overlapped with the αH's of S_4 and T_3. The STD peak intensities of the βH's that were observed were also very weak compared to those of P_6H_β. A STD peak where the γH's of P_6 are centered at showed the largest percent STD (7.1%), though this peak is also overlapped with one of the βH of P_6. According to the saturation transfer difference NMR theory, when a ligand has a binding strength to a protein within the range of $K_d = 10^{-2}$-10^3 μM [17,22,35], the saturation transfer effects on ligand protons directly interacting with the protein are detectable, and that the higher the intensity of the STD peak for a particular ligand proton, the stronger that proton has interaction with the protein that the ligand binds to [35-37]. In the case of the mucin peptide GVTSADD lacking the prolyl residue, we interpreted the result as having no binding protons since there is no STD peak arose corresponding to any of its proton resonances. In tight ligand-receptor binding domain (K_d in nM range) saturation transfer effect is not detected due to slow-exchange of the bound ligand on the NMR time scale which rendered it obsolete of magnetization transfer to the free ligand [42]. The condition is however usually accompanied with proton resonance shifts resulting in spectral characteristic differences between the bound-ligand and free-ligand [42], and in the present case (for GVTSADD) we detected no spectral differences between the free peptide and the peptide mixed with mAb.

The STD data showed that the prolyl residue P_6 is a residue on the peptide GVTSAPD that has stronger interactions with Muc1 monoclonal antibody 6A4 based on STD peak intensities of its protons that were observed, in which P_6 may be viewed as being the critical residue in making contact with Muc1 monoclonal antibody at the antigen binding interface. Furthermore, the interactions between the side chain protons of P_6 and the antibody would be of hydrophobic nature. It is not known what residues line the surface of the antigen binding pocket of mouse Muc1 monoclonal antibody 6A4 used in this study; nonetheless, in a crystal structure of a monoclonal antibody (clone SM3) complexed with a 13-residue peptide TSAPDTRPAPGST, the

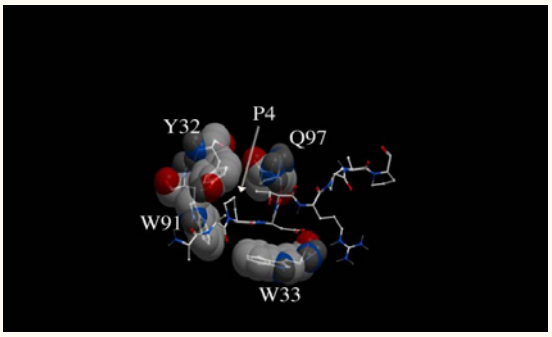

Figure 3 Model of P_4 residue in the peptide TSAPDTRPAPGST binding to monoclonal antibody SM3 in a cleft that is lined with hydrophobic residues, adopted from reference 17. The prolyl ring of P_4 stacks against W_{91} of light chain, while being surrounded by Y_{32} (light chain), W_{33} and Q_{97} of heavy chain. The residue P_6 of GVTSAPD would correspond to the P_4 residue (white dotted arrow) of the peptide on this figure.

residue P_4, which would correspond to P_6 on the peptide tested, has its prolyl ring buried in a hydrophobic pocket formed by Y_{32} and W_{91} of the light chain and W_{33} and Q_{97} of the heavy chain of the SM3 antibody [17]. Figure 3 shows the four residues Y_{32} and W_{91} of light chain, and W_{33} and Q_{97} of heavy chain at the antigen binding pocket of SM3 antibody complexed with the 13-residue mucin peptide, taken from Dokurno et al., 1998 [17], as a model for mucin peptide antigen binding to antiobody. According to this model, the prolyl ring stacks directly against the indole ring of W_{91} (light chain) while being surrounded by Y_{32} (light chain), W_{33} and Q_{97} (heavy chain). The prolyl ring has several van der Waals contacts (~ 4 Å) on either side of it; its αH would be closest to the two indole rings of W_{91} and W_{33}; the βH's closest to the $Q_{97}H_\gamma$'s; the γH's closest to the Y_{32} phenol ring and $Q_{97}H_\gamma$'s; the δH's closest to the Y_{32} phenol ring and W_{91} indole ring [17]. Here, hydrophobic interactions form critical element in mucin peptide-antibody binding, especially, for mucin peptide derived from the VNTR region. The data in this study suggest that the prolyl residue within the sequence tested is a critical residue necessary for antibody binding. We are testing this hypothesis further by substituting P_6 with other hydrophobic residues and aromatic residues on this peptide and conduct further peptide-antibody binding properties of those peptides; their results will be published elsewhere. When designing antigenic peptide model based on the VNTR domain, prolyl residue should be considered an important element for binding. The Muc1 mucin monoclonal antibody 6A4-mucin peptide binding study has implication and relevance in the biological activity of mucin peptides that are to be employed as possible antigenic agents for potential induction of immune responses against them.

CONCLUSIONS

The data showed that a shortened upstream mucin peptide epitope GVTSAPD, even though lacking the full binding sequence PDTRP and contained only one proline in the peptide sequence GVTSAPDTRPAPGSTAPPAH found on the VNTR domain could still bind mAb as revealed by the more pronounced saturation transfer effects (e.g., STD NMR peaks) observed on the side chain protons of P_6 residue and the methyl groups of V_2, T_3 and A_5.

The relatively strong STD NMR peak intensities of the αH, βH's and γH's of P_6 indicate that they interacted stronger with Muc1 monoclonal antibody 6A4 at the antigen binding interface. The same peptide with proline at position 6 substituted for aspartate, more than likely, has no interactions with the antibody. Thus, the P_6 residue on the sequence studied may be evaluated as a critical residue essential for binding. The interactions via the methyl groups of residues V_2, T_3 and A_5 were weaker compared to those found for the γH's of P_6.

ACKNOWLEDGEMENTS

This work was supported by Faculty/Student Collaborative grants and Minority Mentoring grants from the University of Wisconsin-Eau Claire (UWEC) Office of Research and Sponsored Program. We thank the UWEC Chemistry Department for generous support of countless of hours on NMR spectrometer and LC-MS time, and supplies of chemicals.

REFERENCES

1. Singh R, Bandyopadhyay D. MUC1: a target molecule for cancer therapy. Cancer Biol Ther. 2007; 6: 481-486.
2. Gendler SJ. MUC1, the renaissance molecule. J Mammary Gland Biol Neoplasia. 2001; 6: 339-353.
3. Price MR. High molecular weight epithelial mucins as markers in breast cancer. Eur J Cancer Clin Oncol. 1988; 24: 1799-1804.
4. Dent GA, Civalier CJ, Brecher ME, Bentley SA. MUC1 expression in hematopoietic tissues. Am J Clin Pathol. 1999; 111: 741-747.
5. Krüger W, Kröger N, Zander AR. MUC1 expression in hemopoietic tissues. J Hematother Stem Cell Res. 2000; 9: 409-410.
6. McAuley JL, Linden SK, Png CW, King RM, Pennington HL, Gendler SJ, et al. MUC1 cell surface mucin is a critical element of the mucosal barrier to infection. J Clin Invest. 2007; 117: 2313-2324.
7. Ueno K, Koga T, Kato K, Golenbock DT, Gendler SJ, Kai H, et al. MUC1 mucin is a negative regulator of toll-like receptor signaling. Am J Respir Cell Mol Biol. 2008; 38: 263-268.
8. Rahn JJ, Shen Q, Mah BK, Hugh JC. MUC1 initiates a calcium signal after ligation by intercellular adhesion molecule-1. J Biol Chem. 2004; 279: 29386-29390.
9. Meerzaman D, Shapiro PS, Kim KC. Involvement of the MAP kinase ERK2 in MUC1 mucin signaling. Am J Physiol Lung Cell Mol Physiol. 2001; 281: L86-91.
10. Agrawal B, Krantz MJ, Reddish MA, Longenecker BM. Cancer-associated MUC1 mucin inhibits human T-cell proliferation, which is reversible by IL-2. Nat Med. 1998; 4: 43-49.
11. Chan AK, Lockhart DC, von Bernstorff W, Spanjaard RA, Joo HG, Eberlein TJ, et al. Soluble MUC1 secreted by human epithelial cancer cells mediates immune suppression by blocking T-cell activation. Int J Cancer. 1999; 82: 721-726.
12. Kotera Y, Fontenot JD, Pecher G, Metzgar RS, Finn OJ. Humoral immunity against a tandem repeat epitope of human mucin MUC-1 in sera from breast, pancreatic, and colon cancer patients. Cancer Res. 1994; 54: 2856-2860.
13. Ioannides CG, Fisk B, Jerome KR, Irimura T, Wharton JT, Finn OJ. Cytotoxic T cells from ovarian malignant tumors can recognize polymorphic epithelial mucin core peptides. J Immunol. 1993; 151: 3693-3703.
14. Tsang KY, Palena C, Gulley J, Arlen P, Schlom J. A human cytotoxic T-lymphocyte epitope and its agonist epitope from the nonvariable number of tandem repeat sequence of MUC-1. Clin Cancer Res. 2004; 10: 2139-2149.
15. Gendler S, Taylor-Papadimitriou J, Duhig T, Rothbard J, Burchell J. A highly immunogenic region of a human polymorphic epithelial mucin expressed by carcinomas is made up of tandem repeats. J Biol Chem. 1988; 263: 12820-12823.
16. Von Mensdorff-Pouilly S, Moreno M, Verheijen RHM. Natural and Induced Humoral Responses to MUC1. Cancers. 2011; 3: 3073-3103.
17. Dokurno P, Bates PA, Band HA, Stewart LM, Lally JM, Burchell JM, et al. Crystal structure at 1.95 Å resolution of the breast tumour-specific antibody SM3 complexed with its peptide epitope reveals novel hypervariable loop recognition. J Mol Biol. 1998; 284: 713-28.
18. Schuman JT, Grinstead JS, Apostolopoulos V, Campbell AP. Structural and dynamic consequences of increasing repeats in a MUC1 peptide tumor antigen. Biopolymers. 2005; 77: 107-120.
19. Suryanarayanan G, Keifer PA, Wang G, Kinarsky L, Hollingsworth MA, Sherman S. NMR- based Structural Studies of the Glycosylated MUC1 Tandem Repeat Peptide. Int J Mol Sci. 2004; 5: 84-92.
20. Kinarsky L, Suryanarayanan G, Prakash O, Paulsen H, Clausen H, Hanisch FG, et al. Conformational studies on the MUC1 tandem repeat glycopeptides: implication for the enzymatic O-glycosylation of the mucin protein core. Glycobiology. 2003; 13: 929-939.
21. Grinstead JS, Schuman JT, Campbell AP. Epitope mapping of antigenic MUC1 peptides to breast cancer antibody fragment B27.29: a heteronuclear NMR study. Biochemistry. 2003; 42: 14293-14305.
22. Möller H, Serttas N, Paulsen H, Burchell JM, Taylor-Papadimitriou J; Bernd Meyer. NMR-based determination of the binding epitope and conformational analysis of MUC-1 glycopeptides and peptides bound to the breast cancer-selective monoclonal antibody SM3. Eur J Biochem. 2002; 269: 1444-55.
23. Grinstead JS, Koganty RR, Krantz MJ, Longenecker BM, Campbell AP. Effect of glycosylation on MUC1 humoral immune recognition: NMR studies of MUC1 glycopeptide-antibody interactions. Biochemistry. 2002; 41: 9946-9961.
24. Kirnarsky L, Nomoto M, Ikematsu Y, Hassan H, Bennett EP, Cerny RL, et al. Structural analysis of peptide substrates for mucin-type O-glycosylation. Biochemistry. 1998; 37: 12811-12817.
25. Kaiser A, Gaidzik N, Becker T, Menge C, Groh K, Cai H, et al. Fully synthetic vaccines consisting of tumor-associated MUC1 glycopeptides and a lipopeptide ligand of the Toll-like receptor 2. Angew Chem Int Ed Engl. 2010; 49: 3688-3692.
26. Wilkinson BL, Malins LR, Chun CK, Payne RJ. Synthesis of MUC1-lipopeptide chimeras. Chem Commun (Camb). 2010; 46: 6249-6251.
27. Lee DJ, Yang SH, Williams GM, Brimble MA. Synthesis of multivalent Neoglycoconjugates of MUC1 by the conjugation of carbohydrate-centered, triazole-linked glycoclusters to MUC1 peptides using click chemistry. J Org Chem. 2012; 77: 7564-7571.
28. Chan WC, White PD. Basic Procedures. in: Chan WC, White PD, editors. Fmoc Solid Phase Peptide Synthesis, A Practical Approach. Oxford, New York: Oxford University Press. 2000; 41-76.
29. Mant CT, Chen Y, Yan Z, Popa TV, Kovacs JM, Mills JB, et al. HPLC

analysis and purification of peptides. Methods Mol Biol. 2007; 386: 3-55.

30. Trauger SA, Webb W, Siuzdak G. Peptide and Protein analysis with mass spectrometry. Spectroscopy. 2002; 16: 15-28.

31. Berger S, Braun S, editors. in: 200 and More NMR Experiments, A Practical Course. Weinheim, Germany: WILEY-VCH Verlag GmbH & Co. KGaA. 2004; 298-301.

32. TopSpin. v2.0.5, Bruker Corp.

33. The ultimate NMR experience. iNMR.

34. Goddard TD, Kneller DG. SPARKY 3. University of California, San Francisco.

35. Viegas A, Manso J, Nobrega FL, Cabrita EJ. Saturation-Transfer Difference (STD) NMR: A Simple and Fast Method for Ligand Screening and Characterization of Protein Binding. J Chem Educ. 2011; 88: 990-994.

36. Mayer M, Meyer B. Group epitope mapping by saturation transfer difference NMR to identify segments of a ligand in direct contact with a protein receptor. J Am Chem Soc. 2001; 123: 6108-6117.

37. Mayer M, Meyer B. Characterization of Ligand Binding by Saturation Transfer Difference NMR Spectroscopy. Angew Chemie. 1999; 38: 1784-1788.

38. Streiff JH, Juranic NO, Macura SI, Warner DO, Jones KA, Perkins WJ. Saturation transfer difference nuclear magnetic resonance spectroscopy as a method for screening proteins for anesthetic binding. Mol Pharmacol. 2004; 66: 929-935.

39. Victoria Silva Elipe M, Mosley RT, Bednarek MA, Arison BH. 1H-NMR studies on a potent and selective antagonist at human melanocortin receptor 4 (hMC-4R). Biopolymers. 2003; 68: 512-527.

40. Baxter NJ, Williamson MP. Temperature dependence of 1H chemical shifts in proteins. J Biomol NMR. 1997; 9: 359-369.

41. Cierpicki T, Otlewski J. Amide proton temperature coefficients as hydrogen bond indicators in proteins. J Biomol NMR. 2001; 21: 249-261.

42. Wang YS, Liu D, Wyss DF. Competition STD NMR for the detection of high-affinity ligands and NMR-based screening. Magn Reson Chem. 2004; 42: 485-489.

Cite this article

Her C, Westler WM, Yang T (2013) Significance of Proline Residue on Short Mucin Peptide Interactions with Mouse MUC1 Monoclonal Antibody Studied by Saturation Transfer Difference NMR Spectroscopy. JSM Chem 1(1): 1004.